

expressed or absent in gastric foveolar epithelium, intestinal epithelium, hepatocytes, and squamous epithelia.<sup>9</sup> A direct association between CK7 expression and poor prognosis of ESCC patients remains unclear. It has been suggested that because CK7 expression is regulated by the forkhead box A1 (FOXA1) transcription factor, FOXA1 may also regulate several cancer-related genes, such as *LOXL2*, in CK7-positive ESCC cases.<sup>8</sup> It has been also reported that CK7 expression is a statistically significant prognostic factor in patients with stage I and II ESCC.<sup>10</sup> However, the impact of immunohistochemically detected CK7 expression on prognosis or therapeutic outcome in patients with stage I–III ESCC remains unclear.

In the present study, immunohistochemical analysis of CK7 was performed in a large number of primary ESCC samples ( $n = 225$ ). In addition, associations between CK7 expression and therapeutic outcomes in stage II and III ESCC patients were investigated.

## MATERIALS AND METHODS

### *Tissue Samples*

In a retrospective study design, 225 primary tumors were collected from patients diagnosed with ESCC who underwent surgery between 1990 and 2002 at Hiroshima University Hospital (Hiroshima, Japan). All patients underwent curative resection. All patients underwent right transthoracic esophagectomy with extensive lymph node dissection. Reconstruction was performed with a gastric tube positioned in the posterior mediastinum. Only patients without preoperative radiotherapy or chemotherapy and without clinical evidence of distant metastasis were enrolled in the study. Operative mortality was defined as death within 30 days of patients leaving the hospital, and these patients removed from the analysis. Characteristics of the study population are shown in the Supplementary Table 1. The disease-free survival (DFS) median follow-up time was 25 months (range 1–80 months) and the overall survival (OS) median follow-up time was 27 months (range 1–80 months). Postoperative follow-up was scheduled every 1, 2, or 3 months during the first 2 years after surgery and every 6 months thereafter unless more frequent follow-up was deemed necessary. Chest X-ray, chest computed tomographic scan, and serum chemistries were performed at every follow-up visit. Patients were followed by the patients' physician until their death or the date of the last documented contact.

For immunohistochemical analysis, we used archival formalin-fixed, paraffin-embedded tissues. Histologic classification was based on the World Health Organization system. Tumor staging was performed according to the tumor, node, metastasis system stage grouping system.<sup>11</sup>

As a retrospective study where written informed consent was not obtained, identifying information for all samples was removed before analysis for strict privacy protection. These procedures were in accordance with the ethical guidelines for human genome/gene research enacted by the Japanese government. This study was approved by the Ethical Committee for Human Genome Research of Hiroshima University (Hiroshima, Japan).

### *Immunohistochemistry*

One or two representative tumor blocks, including the tumor center, invading front, and tumor-associated non-neoplastic mucosa, was examined from each patient by immunohistochemistry. In cases of large, late-stage tumors, two different sections were examined to include representative areas of the tumor center as well as of the lateral and deep tumor invasive front. Immunohistochemical analysis was performed with a Dako Envision+ Mouse Peroxidase Detection System (Dako Cytomation, Carpinteria, CA). Antigen retrieval was performed by microwave heating in citrate buffer (pH 6.0) for 30 min. Peroxidase activity was blocked with 3% H<sub>2</sub>O<sub>2</sub>–methanol for 10 min, and sections were incubated with normal goat serum (Dako Cytomation) for 20 min to block nonspecific antibody binding sites. Sections were incubated with a mouse monoclonal anti-CK7 antibody (1:50, Clone OV-TL 12/30, Dako Cytomation) for 1 hour at room temperature, followed by incubation with Envision+ anti-mouse peroxidase for 1 hour. For color reaction, sections were incubated with the DAB substrate–chromogen solution (Dako Cytomation) for 10 min. Sections were counterstained with 0.1% hematoxylin. Negative controls were created by omission of the primary antibody.

Expression of CK7 was scored in all tumors as positive or negative. When more than 10% of tumor cells were stained, the immunostaining was considered positive for CK7. By using these definitions, two surgical pathologists (N.O. and K.S.), without knowledge of the clinical and pathologic parameters or the patients' outcomes, independently reviewed immunoreactivity in each specimen. Interobserver differences were resolved by consensus review at a double-headed microscope after independent review.

### *Statistical Methods*

Correlations between clinicopathologic parameters and CK7 expression were analyzed by the chi-square test. Kaplan–Meier survival curves were constructed for CK7-positive and CK7-negative patients. Survival rates were compared between CK7-positive and CK7-negative groups. Differences between survival curves of DFS and OS were tested for statistical significance by the log rank

test. Univariate and multivariate Cox regression was used to evaluate the associations between clinical covariates and DFS or OS. SPSS software was used for these analyses (SPSS, Chicago, IL). Hazard ratio (HR) and 95% confidence interval (CI) were estimated from Cox proportional hazard models. For all analyses, age was treated as a categorical variable (65 years or more vs. less than 65 years). For final multivariable Cox regression models, all variables were included that were moderately associated ( $P < 0.10$ ) with DFS or OS by univariate analysis. A  $P$  value of less than 0.05 was considered statistically significant.

## RESULTS

### *Immunohistochemical Analysis of CK7 in ESCC*

CK7 staining was detected in 55 (24%) of the 225 ESCC specimens investigated. In the nonneoplastic esophageal mucosa adjacent to the tumor, no CK7 staining was observed in squamous epithelial and stromal cells. As reported previously, the esophageal gland was stained by CK7 (Fig. 1a)<sup>12</sup>. Of the 55 ESCC cases in which CK7 staining was detected, 35 cases showed only weak staining of the cytoplasm of tumor cells. In 20 ESCC cases, strong staining was observed in the cytoplasm of tumor cells (Fig. 1b). Expression of CK7 was observed in some cases of squamous cell carcinoma-in-situ (Fig. 1c). When more than 10% of tumor cells were stained, the immunostaining was considered positive for CK7. In total, 20 (9%) of 225 ESCC cases were positive for CK7. We analyzed the

relationship between CK7 expression and clinicopathologic characteristics. CK7-positive ESCC cases were more advanced in terms of T classification ( $P = 0.0014$ ,  $\chi^2$  test), N classification ( $P = 0.0195$ ,  $\chi^2$  test), and tumor stage ( $P = 0.0016$ ,  $\chi^2$  test) than CK7-negative ESCC cases (Table 1). Expression of CK7 was not associated with age, sex, or histologic classification.

### *Relationship Between CK7 Staining and Prognosis of Patients with Stage 0–III ESCC*

The association between CK7 expression and DFS or OS was investigated by Kaplan–Meier analysis in all ESCC samples (stage 0–III,  $n = 225$ ). We found that CK7 expression was significantly associated with both poorer DFS and OS ( $P = 0.0044$  and  $P = 0.0075$ , log rank test, respectively; Fig. 2a). Univariate and multivariate Cox proportional hazards analysis was used to further evaluate the association between CK7 expression and DFS (Supplementary Table 2) or OS (Supplementary Table 3). The univariate analysis indicated that expression of CK7 (HR 2.72; 95% CI 1.32–5.59;  $P = 0.0066$ ), tumor stage (HR 13.89; 95% CI 5.03–38.46;  $P < 0.0001$ ), and adjuvant chemotherapy (HR 1.88; 95% CI 1.07–3.32;  $P = 0.0293$ ) were associated with DFS while age, sex, or histologic classification were not. We next performed multivariate model, which included CK7 expression, tumor stage, and adjuvant chemotherapy. However, CK7 expression was not an independent prognostic indicator of DFS (HR 2.01; 95% CI 0.97–4.17;  $P = 0.0616$ ). The univariate analysis

**FIG. 1** Immunohistochemical analysis of CK7 in ESCC tissues. In the nonneoplastic esophageal mucosa adjacent to the tumor, esophageal glands were stained by CK7, but squamous epithelium was negative (a) (original magnification, 100 $\times$ ). Strong and extensive staining was observed in the cytoplasm of ESCC cells (b) (original magnification, 400 $\times$ ). Expression of CK7 was observed in some cases of squamous cell carcinoma-in-situ (c) (original magnification, 200 $\times$ )

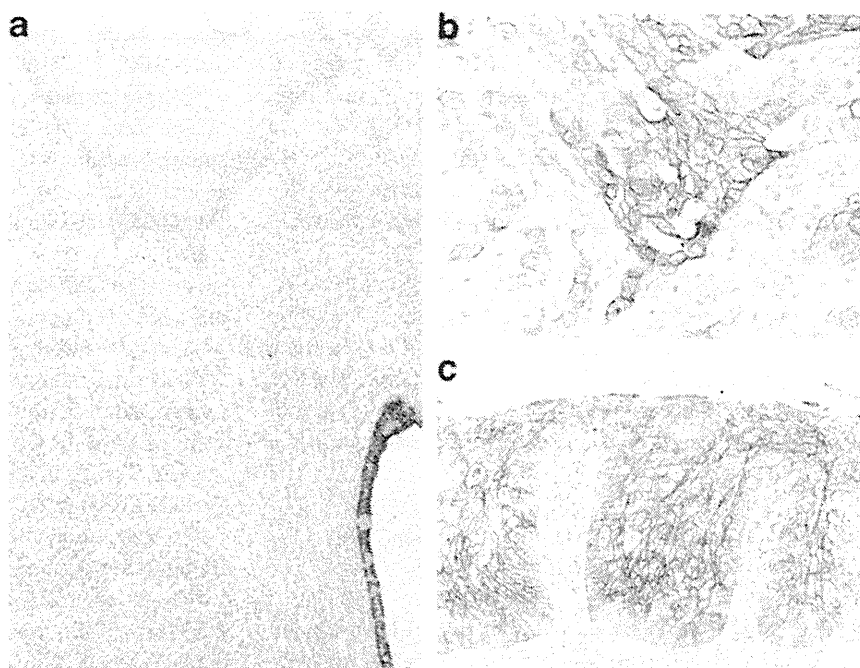


**TABLE 1** Relationship between cytokeratin 7 (CK7) expression and clinicopathologic characteristics in esophageal squamous cell carcinoma

Characteristic	CK7 expression		<i>P</i> <sup>a</sup>
	Positive (%)	Negative	
Age			
<66 years	8 (7)	104	0.4832
≥66 years	12 (11)	101	
Sex			
Male	17 (9)	178	0.7360
Female	3 (10)	27	
T classification			
Tis/1	6 (5)	121	0.0014
T2	1 (5)	21	
T3	12 (16)	62	
T4	1 (50)	1	
N classification			
N0	6 (30)	14	0.0195
N1	120 (59)	85	
Tumor stage			
0/I	4 (4)	97	0.0016
II	5 (8)	60	
III	11 (19)	48	
Histologic classification			
Well/moderate	16 (10)	151	0.7890
Poor	4 (7)	54	

<sup>a</sup>  $\chi^2$  test

indicated that expression of CK7 (HR 2.70; 95% CI 1.26–5.78;  $P = 0.0110$ ) and tumor stage (HR 17.24; 95% CI 5.32–55.56;  $P < 0.0001$ ) were associated with OS, while age, sex, and histologic classification were not. Adjuvant chemotherapy was moderately associated with OS (HR 1.81; 95% CI 0.99–3.33;  $P = 0.0562$ ). We also performed multivariate model, which included CK7 expression, tumor stage, and adjuvant chemotherapy. CK7 expression was an independent prognostic indicator of OS (HR 2.24; 95% CI 1.03–4.88;  $P = 0.0426$ ).

We performed survival analysis with other cutoff point. When more than 25% of tumor cells were stained, the immunostaining was considered positive for CK7. In stage 0–III ESCC cases, 9 (4%) of 225 ESCC cases were positive for CK7, and similar results were obtained (data not shown). These results demonstrate that CK7 expression is a useful predictor of OS.

#### Relationship Between CK7 Staining and Prognosis of Patients with Stage II and III ESCC

Patients with ESCC at stage 0 and stage I have a good rate of survival, whereas patients with ESCC at stage IV

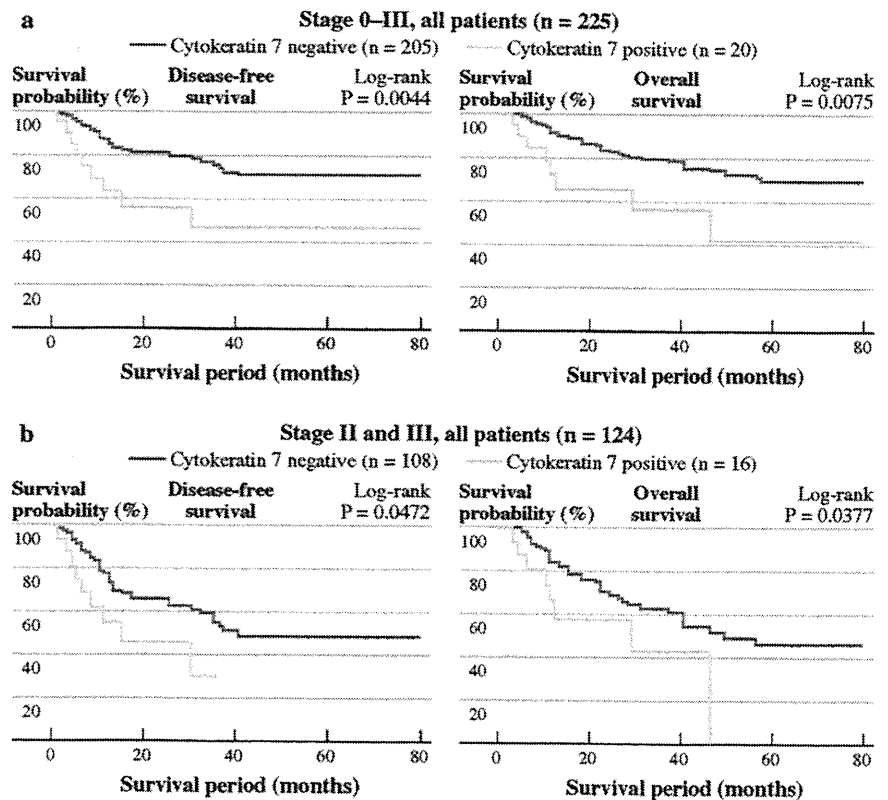
show a poor rate of survival. However, it is difficult to predict the survival of patients with stage II or stage III ESCC, and these patients would benefit the most from prognostic biomarkers. Therefore, we analyzed the prognostic value of CK7 expression in patients with stage II and III ESCC ( $n = 124$ ). In Kaplan–Meier analysis, we found that CK7 expression was significantly associated with both poorer DFS and OS (respectively,  $P = 0.0472$  and  $P = 0.0377$ , log rank test; Fig. 2b). Because adjuvant chemotherapy for patients with stage II and stage III ESCC influences survival, we analyzed individuals who did not receive adjuvant chemotherapy ( $n = 73$ ). We found that CK7 expression was significantly associated with both poorer DFS and OS in stage II and III ESCC patients who did not receive adjuvant chemotherapy (respectively,  $P = 0.0008$  and  $P = 0.0003$ , log rank test; Fig. 3a).

To evaluate the potential for CK7 expression as a prognostic predictor in patients with stage II and III ESCC, both univariate and multivariate Cox proportional hazards analyses were used to further evaluate the association of CK7 expression with DFS (Table 2) or OS (Table 3). In univariate analysis, CK7 expression (HR 2.05; 95% CI 0.99–4.27;  $P = 0.0548$ ) was moderately associated with DFS. We next performed multivariate model, which included CK7 expression and the tumor stage. However, CK7 expression was not an independent prognostic classifier of DFS (HR 1.77; 95% CI 0.85–3.70;  $P = 0.1297$ ). In univariate analysis, CK7 expression (HR 2.22; 95% CI 1.02–4.83;  $P = 0.0450$ ) and tumor stage (HR 2.97; 95% CI 1.57–5.62;  $P = 0.0008$ ) were associated with OS. We also performed multivariate model, which included CK7 expression and the tumor stage. CK7 expression was an independent prognostic predictor of OS (HR 2.25; 95% CI 1.01–5.00;  $P = 0.0474$ ).

We performed survival analysis with other cutoff point. When more than 25% of tumor cells were stained, the immunostaining was considered positive for CK7. In stage II and III ESCC cases, 7 (6%) of 124 cases were positive for CK7, and similar results were obtained (data not shown).

Because CK7 staining was detected in ESCC in situ, we analyzed the prognostic value of CK7 expression in patients with stage 0 and stage I ESCC ( $n = 101$ ). When more than 10% of tumor cells were stained, the immunostaining was considered positive for CK7. In total, 4 (4%) of 101 cases were positive for CK7. CK7 expression was not associated with DFS or OS in Kaplan–Meier analysis (data not shown). We also performed survival analysis with another cutoff point. When more than 25% of tumor cells were stained, the immunostaining was considered positive for CK7. In total, 2 (2%) of 101 ESCC cases were positive for CK7. However, CK7 expression was not associated with DFS or OS in Kaplan–Meier analysis (data not shown).

**FIG. 2** Disease-free survival and overall survival of patients with ESCC. Kaplan–Meier curves of a CK7-positive or CK7-negative ESCC in stage 0–III patients and of b patients with stage II and III disease



These results indicate that CK7 expression is associated with OS but not DFS in patients with stage II and III ESCC.

*Efficacy of Adjuvant Chemotherapy in CK7-Positive and CK7-Negative Patients*

*CK7 Expression and Therapeutic Outcome*

Biomarkers that can predict therapeutic outcomes may provide tools to allow physicians to better stratify patients to more effective treatments. We analyzed associations between CK7 expression and therapeutic outcomes in stage II and III ESCC patients. Information regarding the administration of adjuvant chemotherapy was available for all patients. Chemotherapy regimens were primarily 5-fluorouracil based. In stage II and III ESCC patients who received adjuvant chemotherapy ( $n = 51$ ), adjuvant chemotherapy was not found to be beneficial. Furthermore, CK7 expression was not significantly associated with therapeutic outcome in patients with stage II and III ESCC (Fig. 3b). These results indicate that CK7 expression cannot predict therapeutic outcome in patients with stage II and III ESCC.

Although we performed survival analysis with another cutoff point, CK7-positive cases were not found in patients who received adjuvant chemotherapy when the cutoff value was set at 25%. Therefore, we set cutoff value at 10% in the following analysis.

We have demonstrated that CK7 expression has the potential to identify patients at high risk of cancer-specific mortality. Furthermore, our data have demonstrated that CK7-positive cases had significantly worse cancer-specific mortality than CK7-negative cases in stage II and III ESCC patients who did not receive adjuvant chemotherapy. These results indicate that CK7 expression is associated with a more aggressive histology of the primary tumor. Because CK7-positive ESCC cases had significantly worse cancer-specific mortality than CK7-negative ESCC cases, adjuvant chemotherapy may be indicated for patients with CK7-positive ESCC. However, it is unclear whether such patients may benefit from adjuvant chemotherapy. To address this issue, we examined whether CK7 expression can identify patients for whom adjuvant chemotherapy is beneficial in stage II and III ESCC. Although in patients with CK7-positive ESCC ( $n = 16$ ) there is a trend toward improved survival with the use of adjuvant chemotherapy in CK7-positive ESCC, therapeutic outcome between patients with CK7-positive and CK7-negative ESCC was not significantly different (Fig. 3c). Conversely, CK7-negative patients with ESCC ( $n = 108$ ) did not benefit

**FIG. 3** Disease-free survival and overall survival of patients with stage II and III ESCC. Kaplan–Meier curves of CK7-positive or CK7-negative ESCC in stage II and III ESCC patients who did not receive adjuvant chemotherapy (a); stage II and III patients who received adjuvant chemotherapy (b); stage II and III CK7-positive ESCC patients with or without adjuvant chemotherapy (c); stage II and III CK7-negative ESCC patients with or without adjuvant chemotherapy (d)

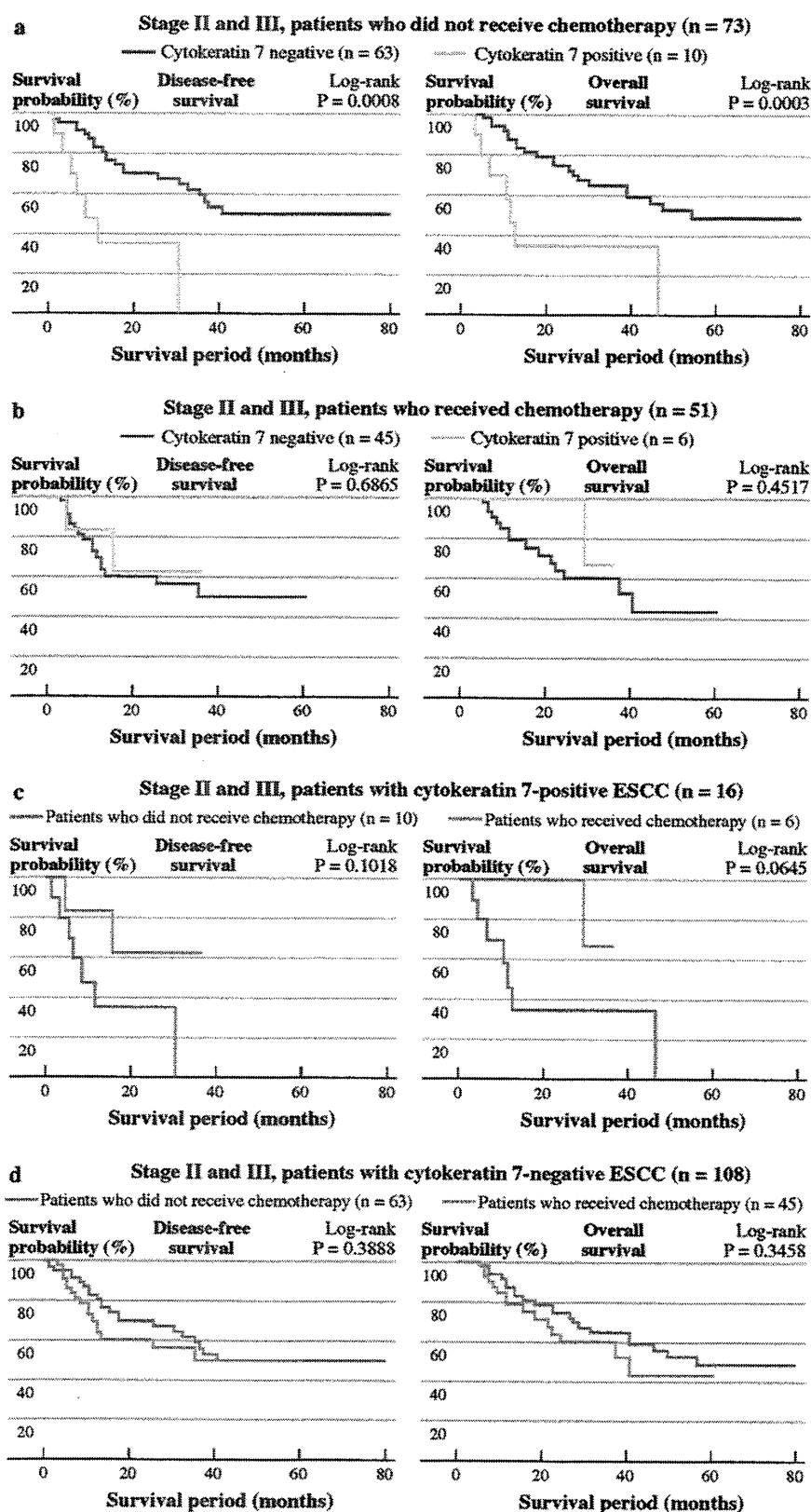


**TABLE 2** Univariate and multivariate Cox regression analysis of CK7 expression and disease-free survival in esophageal squamous cell carcinoma (stage II and III,  $n = 124$ )

Characteristic	MST, mo	Univariate analysis		Multivariate analysis	
		HR (95% CI)	<i>P</i>	HR (95% CI)	<i>P</i>
CK7 expression					
Negative	40	1 (Ref.)	0.0548	1 (Ref.)	0.1297
Positive	15	2.05 (0.99–4.27)		1.77 (0.85–3.70)	
Tumor stage					
II	NR	1 (Ref.)	0.0018	1 (Ref.)	0.0032
III	15	2.57 (1.42–4.65)		2.46 (1.35–4.46)	
Adjuvant chemotherapy					
Not received	NR	1 (Ref.)	0.8933		
Received	36	1.04 (0.58–1.86)			
Age					
≥66 years	NR	1 (Ref.)	0.5596		
<66 years	32	1.19 (0.67–2.10)			
Sex					
Female	NR	1 (Ref.)	0.1324		
Male	35	2.46 (0.76–7.94)			
Histologic classification					
Well/moderate	NR	1 (Ref.)	0.3023		
Poor	32	1.37 (0.75–2.50)			

CK7 Cytokeratin 7, HR hazard ratio, CI confidence interval, NR not reached, MST median survival time

**TABLE 3** Univariate and multivariate Cox regression analysis of CK7 expression and overall survival in esophageal squamous cell carcinoma (stage II and III,  $n = 124$ )

Characteristic	MST, mo	Univariate analysis		Multivariate analysis	
		HR (95% CI)	<i>P</i>	HR (95% CI)	<i>P</i>
CK7 expression					
Negative	49	1 (Ref.)	0.0450	1 (Ref.)	0.0474
Positive	29	2.22 (1.02–4.83)		2.25 (1.01–5.00)	
Tumor stage					
II	NR	1 (Ref.)	0.0008	1 (Ref.)	0.0018
III	46	2.97 (1.57–5.62)		2.98 (1.50–5.92)	
Adjuvant chemotherapy					
Not received	46	1 (Ref.)	0.9433		
Received	40	1.02 (0.55–1.91)			
Age					
≥66 years	NR	1 (Ref.)	0.6711		
<66 years	46	1.19 (0.65–2.17)			
Sex					
Female	NR	1 (Ref.)	0.2134		
Male	46	2.11 (0.65–6.80)			
Histologic classification					
Well/moderate	49	1 (Ref.)	0.2689		
Poor	37	1.41 (0.76–2.62)			

CK7 Cytokeratin 7, HR hazard ratio, CI confidence interval, NR not reached, MST median survival time

from adjuvant chemotherapy (Fig. 3d). These results demonstrate the potential for the use of CK7 immunohistochemistry to identify patients who can benefit from adjuvant chemotherapy.

## DISCUSSION

The long-term survival of patients with ESCC remains poor as a result of the high incidence of lymph node metastasis and early recurrence after curative surgical resection. In the present study, we performed immunohistochemical analysis of CK7 in 225 ESCC cases. Univariate and multivariate analyses revealed that CK7 expression is an independent prognostic classifier of OS in stage 0–III ESCC. We previously reported that patients with CK7-positive ESCC have a worse prognosis for stage I and II ESCC in a cohort from the National Cancer Center Hospital East (Kashiwa, Japan).<sup>10</sup> Therefore, the usefulness of CK7 immunohistochemical analysis is now shown in two independent cohorts. Taken together, these results indicate that immunohistochemical analysis of CK7 is a clinically useful method for prediction of survival of patients with ESCC.

Patients diagnosed with stage II or stage III ESCC have variable prognoses. These groups would benefit from the discovery of prognostic markers that identify individuals for whom adjuvant treatment would be advantageous. In the present study, we demonstrated that CK7 expression was associated with the OS of patients with stage II and stage III ESCC. This indicates that immunohistochemical analysis of CK7 may help identify patients with a high risk of disease recurrence. In the present study, CK7 expression was associated with DFS and OS in stage II and III ESCC patients who did not receive adjuvant chemotherapy. In contrast, CK7 expression was not associated with therapeutic outcome in patients with stage II and III ESCC who received adjuvant chemotherapy. These results suggest that adjuvant chemotherapy may improve survival of patients with CK7-positive ESCC. Although there is a trend toward improved survival with the use of adjuvant chemotherapy in CK7-positive ESCC, therapeutic outcome between patients with CK7-positive and CK7-negative ESCC was not significantly different. As the number of CK7-positive stage II and III ESCC cases was small ( $n = 16$ ), this result should be further investigated in a large ESCC cohort.

The mechanisms underlying the associations between CK7 expression and patients' survival remains unclear. It has been suggested that CK7 expression may be regulated by the FOXA1 transcription factor because *KRT7* mRNA expression levels correlate with *FOXA1* mRNA expression levels.<sup>8</sup> In the TE3 esophageal cancer cell line, knockdown of FOXA1 by siRNA inhibits cell migration and CK7

expression.<sup>8</sup> Therefore, CK7 may be a marker for ESCC expressing FOXA1, and some genes induced by FOXA1 may be associated with cell migration. In addition to CK7, immunohistochemical analysis of FOXA1 may also have the potential to predict patient survival. In the present study, there is a trend toward improved survival with the use of adjuvant chemotherapy in CK7-positive ESCC. To our knowledge, a direct association between CK7 and chemotherapy efficacy has not been investigated. It is possible that some genes induced by FOXA1 may enhance the efficacy of adjuvant chemotherapy in ESCC.

In summary, we have shown that CK7 expression is an independent prognostic classifier in patients with ESCC. Furthermore, there is a trend toward improved survival with the use of adjuvant chemotherapy in CK7-positive ESCC. It is possible that immunohistochemical analysis of CK7 may help identify patients who would benefit from adjuvant chemotherapy. Identification of FOXA1 target genes may improve our understanding of the characteristics of CK7-positive ESCC.

**ACKNOWLEDGMENT** We thank Shinichi Norimura for his technical assistance and advice. This work was carried out with the cooperation of the Research Center for Molecular Medicine of the Faculty of Medicine of Hiroshima University. We thank the Analysis Center of Life Science of Hiroshima University for the use of their facilities. This work was supported in part by grants-in-aid for Cancer Research from the Ministry of Education, Culture, Science, Sports and Technology of Japan and in part by a grant-in-aid for the Third Comprehensive 10-Year Strategy for Cancer Control from the Ministry of Health, Labor and Welfare of Japan, and by the National Institute of Biomedical Innovation (Program for Promotion of Fundamental Studies in Health Sciences) and by National Cancer Center Research and Development Fund.

## REFERENCES

1. IARC 2003 Oesophageal cancer. In: Stewart BW, Kleihues P (eds) World cancer report. Lyon: IARC Press, pp. 223–7.
2. Goseki N, Koike M, Yoshida M. Histopathologic characteristics of early stage esophageal carcinoma. A comparative study with gastric carcinoma. *Cancer*. 1992;69:1088–93.
3. Courrech Staal EF, van Coevorden F, Cats A, Aleman BM, van Velthuysen ML, Boot H et al. Outcome of low-volume surgery for esophageal cancer in a high-volume referral center. *Ann Surg Oncol*. 2009;16:3219–26.
4. Takeno S, Noguchi T, Kikuchi R, Uchida Y, Yokoyama S, Müller W. Prognostic value of cyclin B1 in patients with esophageal squamous cell carcinoma. *Cancer*. 2002;94:2874–81.
5. Noguchi T, Oue N, Wada S, Sentani K, Sakamoto N, Kikuchi A et al. h-Prune is an independent prognostic marker for survival in esophageal squamous cell carcinoma. *Ann Surg Oncol*. 2009;16:1390–6.
6. Isohata N, Aoyagi K, Mabuchi T, Daiko H, Fukaya M, Ohta H et al. Hedgehog and epithelial-mesenchymal transition signaling in normal and malignant epithelial cells of the esophagus. *Int J Cancer*. 2009;125:1212–21.
7. Sakamoto N, Oue N, Noguchi T, Sentani K, Anami K, Sanada Y, et al. Serial analysis of gene expression of esophageal

- squamous cell carcinoma: ADAMTS16 is upregulated in esophageal squamous cell carcinoma. *Cancer Sci.* 2010;101:1038–44.
8. Sano M, Aoyagi K, Takahashi H, Kawamura T, Mabuchi T, Igaki H, et al. Forkhead box A1 transcriptional pathway in KRT7-expressing esophageal squamous cell carcinomas with extensive lymph node metastasis. *Int J Oncol.* 2010;36:321–30.
  9. Moll R, Divo M, Langbein L. The human keratins: biology and pathology. *Histochem Cell Biol.* 2008;129:705–33.
  10. Yamada A, Sasaki H, Aoyagi K, Sano M, Fujii S, Daiko H, et al. Expression of cytokeratin 7 predicts survival in stage I/IIA/IIB squamous cell carcinoma of the esophagus. *Oncol Rep.* 2008;20:1021–7.
  11. Sobin LH, Wittekind CH, editors. TNM classification of malignant tumors. 6th ed. New York: Wiley-Liss, 2002:60–4.
  12. Haleem A, Kfoury H, Al Juboury M, Al Hussein H. Paget's disease of the oesophagus associated with mucous gland carcinoma of the lower oesophagus. *Histopathology.* 2003;42:61–5.



## Regression of rectal MALT lymphoma after antibiotic treatment in a patient negative for *Helicobacter pylori*

E. Ohara · Y. Kitadai · M. Onoyama · M. Ohnishi ·  
K. Shinagawa · S. Oka · S. Yoshida · S. Tanaka ·  
N. Sakamoto · W. Yasui · F. Shimamoto · K. Chayama

Received: 17 August 2011 / Accepted: 10 October 2011  
© Springer 2011

**Abstract** A 53-year-old man was referred to our hospital with bloody stool. Barium enema study and colonoscopy revealed multiple small nodules on the anterior wall of the lower rectum. Biopsy specimens showed proliferation of atypical lymphoid cells forming the nodules. Mucosa-associated lymphoid tissue lymphoma was diagnosed on the basis of histologic and immunohistochemical examinations. No metastasis was detected in lymph nodes or distant organs, indicative of clinical stage I disease. Although the test results were negative for *Helicobacter pylori*, eradication therapy was performed. The lesion disappeared completely within 9 months after the triple antibiotic therapy. *H. pylori* eradication therapy may be a useful treatment option regardless of *H. pylori* status.

**Keywords** Rectal MALT lymphoma · *Helicobacter pylori* · Eradication

E. Ohara · Y. Kitadai (✉) · M. Onoyama · M. Ohnishi ·  
K. Shinagawa · K. Chayama  
Department of Gastroenterology and Metabolism, Hiroshima  
University Graduate School of Biomedical Science,  
1-2-3 Kasumi, Minami-ku, Hiroshima 734-8551, Japan  
e-mail: kitadai@hiroshima-u.ac.jp

S. Oka · S. Yoshida · S. Tanaka  
Department of Endoscopy, Hiroshima University Hospital,  
Hiroshima, Japan

N. Sakamoto · W. Yasui  
Department of Molecular Pathology, Hiroshima University  
Graduate School of Biomedical Science, Hiroshima, Japan

F. Shimamoto  
Department of Health Science, Faculty of Human Culture and  
Society, Prefectural University of Hiroshima, Hiroshima, Japan

### Introduction

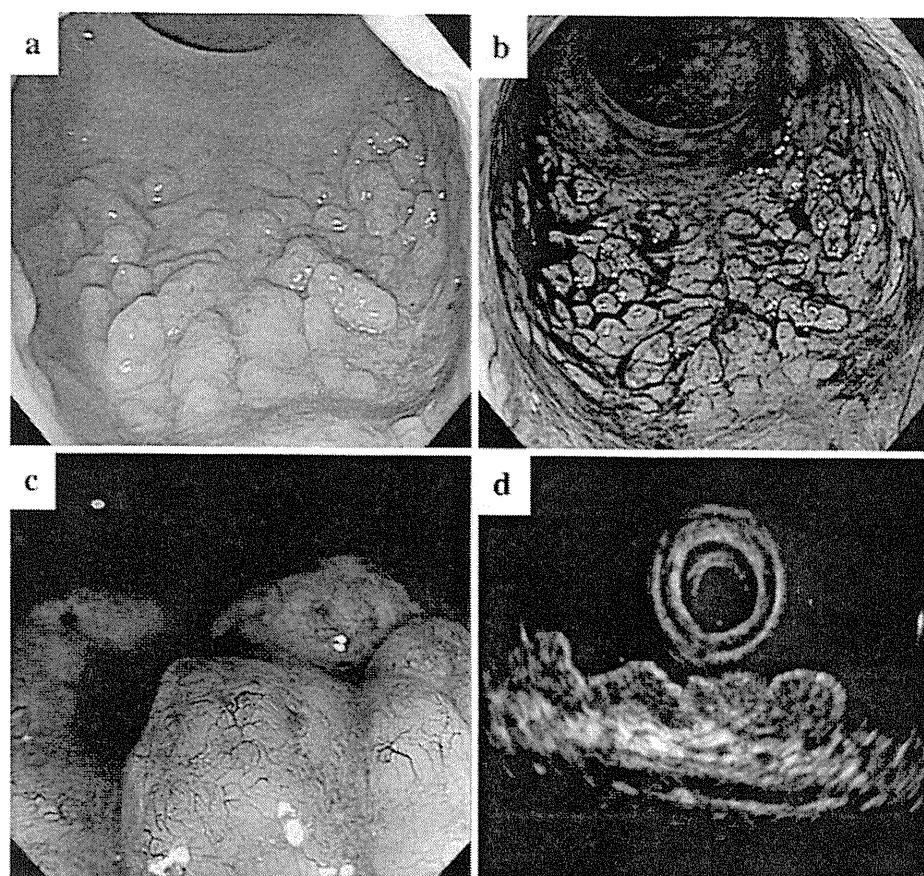
Mucosa-associated lymphoid tissue (MALT) lymphoma was first described by Isaacson and Wright in 1983 [1, 2]. Extranodal marginal zone lymphoma of MALT are frequently found in the gastrointestinal tract, with most such lymphomas arising in the stomach. Those arising in the stomach have been shown to be closely related to *H. pylori* infection [3–5]. Colorectal lymphomas account for only 5–10% of all gastrointestinal lymphomas. The ileocecum and rectum are favorite sites of colorectal lymphoma [6]. Primary rectal MALT lymphoma is rare, and treatment of rectal MALT lymphoma has not been as well studied as treatment of gastric MALT lymphoma. There is no established standard therapy for rectal MALT lymphoma, but several recent reports have documented disappearance of rectal MALT lymphoma by *Helicobacter pylori* (*H. pylori*) eradication therapy [7–19].

Herein, we describe a case in which complete remission of rectal MALT lymphoma was achieved by triple antibiotic therapy in an *H. pylori*-negative patient. We review the literature and speculate on possible standardization of *H. pylori* eradication therapy for cases of rectal MALT lymphoma.

### Case report

A 53-year-old man was referred to Hiroshima University Hospital on December 2007 with a history of persistent bloody stool. Physical examination upon admission revealed no abnormalities. Colonoscopy revealed that the multiple small nodules formed a spreading flat mass on the anterior wall of the lower rectum (Fig. 1a, b). Magnified chromoendoscopy and magnified narrow band imaging

**Fig. 1** Endoscopic images obtained before the triple antibiotic treatment. The lesion consisted of multiple small nodules and formed a spreading flat mass on the anterior wall of rectum (a, b). Magnified endoscopy and magnified narrow band imaging revealed a partial disappearance of normal pit pattern with abnormal vascular vessels on the nodules (c). Endoscopic ultrasonography revealed thickening of the second mucosal layer (d)

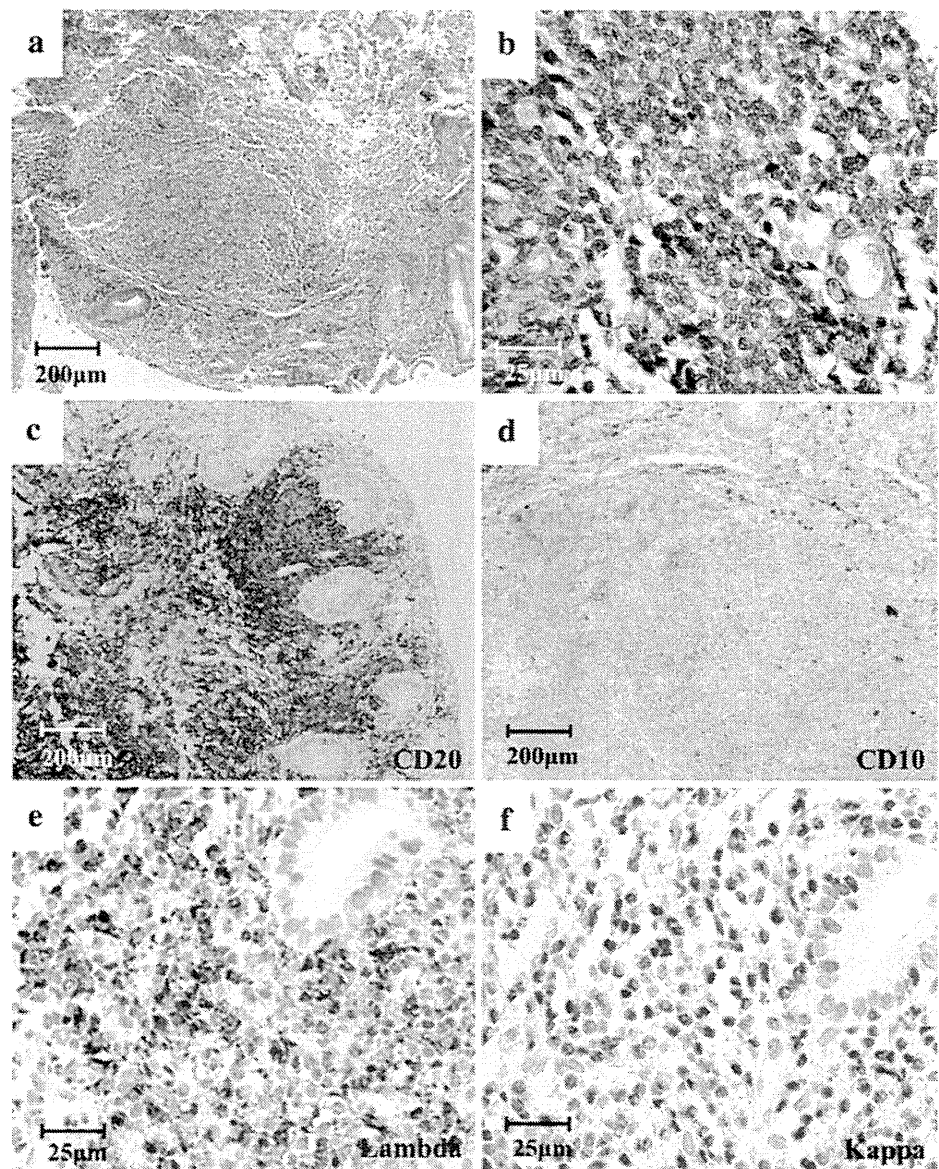


revealed a partial disappearance of normal pit pattern and normal vascular network on the nodules (Fig. 1c). Endoscopic ultrasonography, performed with a 20-MHz probe, showed thickening of the hypoechoic second mucosal layer (Fig. 1d). Proliferation of small atypical lymphoid cells forming the nodules was evident on biopsy specimens. These nodules were located in the mucosal and submucosal layers (Fig. 2a) and invaded and destroyed the epithelium to form lymphoepithelial lesions (Fig. 2b). Immunohistochemistry revealed that the atypical lymphoid cells were positive for B-cell markers (CD20) (Fig. 2c) but negative for T-cell markers (CD3, CD5, CD45RO) (not shown) and CD10 (Fig. 2d), cyclin D1 (not shown). The proliferation rate was about 10% as assessed by Ki-67 staining (not shown). To rule out inflammatory change, immunohistochemistry for immunoglobulin light chain  $\kappa/\lambda$  was performed. The immunoglobulin light chain  $\lambda/\kappa$  ratio was above 10, indicating  $\lambda$  light chain restriction and monoclonal B-cell proliferation (Fig. 2e, f). Immunoglobulin light chain gene rearrangement was detected by a polymerase chain reaction using formalin-fixed, paraffin embedded tissue samples. API2-MALT1 chimeric transcript was not detected by reverse transcriptase polymerase chain reaction using

frozen specimens. Low-grade MALT lymphoma was diagnosed on the basis of the histopathologic and phenotypic characteristics. Upper gastrointestinal endoscopy revealed normal gastric mucosa without atrophic change. Capsule endoscopy, abdominal computed tomography, bone marrow biopsy, and gallium scintigraphy were also performed, and no metastatic lesions were detected, indicative of clinical stage I (Lugano staging system) disease.

*H. pylori* infection was evaluated by anti-*H. pylori* IgG antibody serology, urea breath test, and *H. pylori* culture of biopsy specimens from the gastric mucosa. Although there was no evidence of *H. pylori* infection, we selected *H. pylori* eradication therapy as first-line treatment because MALT lymphoma is slow to spread, and *H. pylori* eradication therapy has few side effects. Triple therapy was used: oral rabeprazole at 20 mg/day, oral amoxicillin (AMPC) at 1500 mg/day, and oral clarithromycin (CAM) at 400 mg/day, all for 7 days. After *H. pylori* eradication, lesion nodularity gradually decreased; the lesion disappeared completely within 9 months after the eradication therapy (Fig. 3). Complete remission was confirmed by histologic examination. The patient remains in complete remission, now 3 years after treatment.

**Fig. 2** Histologic features of the biopsy specimens. H&E staining revealed moderate proliferation of atypical lymphoid cells forming nodules (a) that were located in the mucosal and submucosal layers. Immunohistochemical analysis revealed that the atypical lymphoid cells were positive for CD20/CD79a and negative for CD10 (c, d). Lymphoepithelial lesions were also detected (b). The immunoglobulin light chain  $\lambda/\kappa$  ratio was above 10, indicating B-cell monoclonality (e, f)



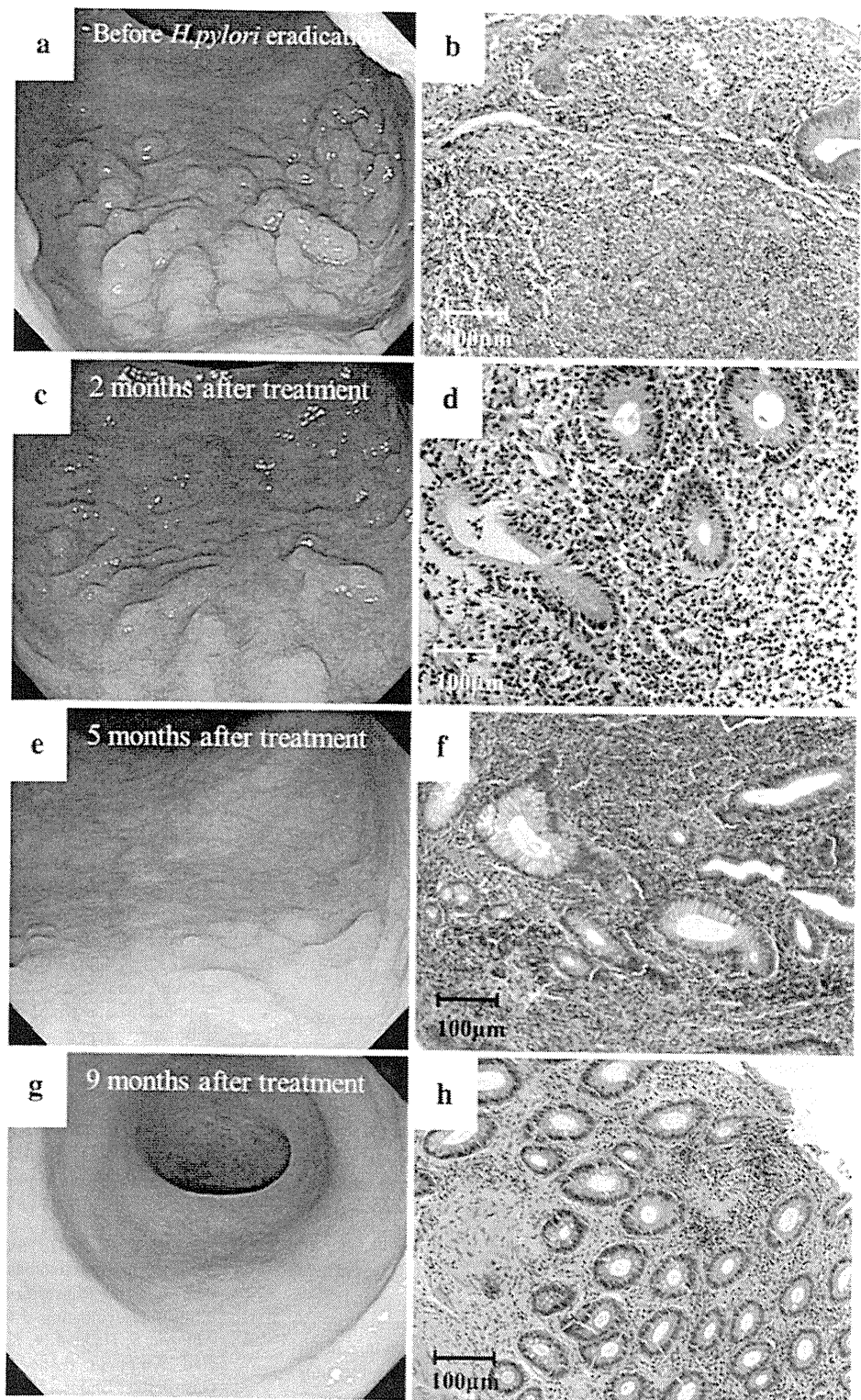
## Discussion

Regression of gastric MALT lymphoma after successful *H. pylori* eradication has been consistently reported [3]; however, it is unclear whether *H. pylori* eradication therapy is effective for colorectal MALT lymphoma. Therapeutic options for rectal MALT lymphoma include chemotherapy, radiotherapy, and surgical or endoscopic resection [7, 8]. Grunberger et al. [9] reported 45% positivity (35 of 77 cases) for *H. pylori* among MALT lymphomas (not including primary gastric MALT lymphomas). Eradication therapy was effective for only 1 of 16 *H. pylori*-positive cases. Ahlawat et al. [7] summarized 30 cases of primary rectal MALT lymphoma. Only 7 of the 30 patients were infected with *H. pylori*. The majority

of patients underwent curative surgical or endoscopic resection.

The effectiveness of *H. pylori* eradication therapy for rectal MALT lymphoma in a patient positive for *H. pylori* was first reported by Matsumoto et al. in 1997 [10, 11]. Inoue et al. [12] reported a patient without *H. pylori* infection in whom rectal MALT lymphoma regressed after antibiotic treatment. Niino et al. [13] reported that 5 of 8 cases of rectal MALT lymphoma regressed after antibiotic treatment. We conducted a MEDLINE search for English-language articles pertaining to treatment of rectal MALT lymphoma with antibiotics. Reported cases of regression after such treatment are summarized in Table 1 [14–18]. There were 2 men and 12 women with a mean age of 65.9 years (range 33–83 years). Eight out of the 14 patients were negative for

**Fig. 3** After *H. pylori* eradication therapy, nodularity of the lesion decreased gradually, and the lesion disappeared completely within 9 months of therapy. Complete remission was confirmed by histologic examination. **a, b** Before *H. pylori* eradication therapy. **c, d** 2 months after treatment. **e, f** 5 months after treatment. **g, h** 9 months after treatment



*H. pylori* infection, but the rectal MALT lymphoma lesions disappeared within 1 year after the antibiotic therapy. Dohden et al. [19] reported that a new quinolone antibiotic was effective for rectal MALT lymphoma. Although the

mechanism underlying regression of rectal MALT lymphoma after antibiotic treatment remains unclear, it is possible that antigenic stimuli from an unknown bacterium plays a role in the pathogenesis of rectal MALT lymphoma.



**Table 1** Reported cases of regression of rectal MALT lymphomas after *H. pylori* eradication therapy

	Year	Reference	Patient	Drugs	Therapeutic effect	Observation period (month)
<i>H. pylori</i> positive	1997	Matsumoto et al. [10]	72-year-old woman	PAC	Disappearance	0.75
	2004	Hori et al. [16]	83-year-old woman	PACMG	Disappearance	1
	2004	Dohden et al. [19]	60-year-old woman	L	Disappearance	(-)
	2010	Niino et al. [13]	67-year-old woman	AC	Disappearance	(-)
	2010	Niino et al. [13]	68-year-old woman	AC	Disappearance	(-)
	2010	Niino et al. [13]	80-year-old woman	AC	Disappearance	(-)
<i>H. pylori</i> negative	1999	Inoue and Chiba [12]	62-year-old woman	PAC	Disappearance	1
	2002	Nakase et al. [15]	66-year-old woman	PAMT	Disappearance	5
	2002	Nakase et al. [15]	33-year-old woman	AC	Disappearance	1
	2002	Hisabe et al. [14]	70-year-old woman	PAC	Disappearance	0.3
	2005	Kikuchi et al. [17]	80-year-old woman	PAC	Partial regression	6
	2005	Kikuchi et al. [17]	71-year-old man	AC	Disappearance	12
	2005	Ahlawat et al. [18]	57-year-old woman	PAC	Disappearance	12
	2011	Ohara (here in reported)	53-year-old man	PAC	Disappearance	9

*P* proton pump inhibitor, *A* amoxicillin, *C* clarithromycin, *M* metronidazole, *T* tetracycline, *G* gatifloxacin, *L* levofloxacin, (-) not described

In conclusion, we observed dramatic endoscopic and histologic changes in rectal MALT lymphoma within a short period after antibiotic therapy. Further studies are needed to clarify the mechanisms responsible for the effectiveness of antibiotic treatment and to establish a standard treatment protocol for rectal MALT lymphoma.

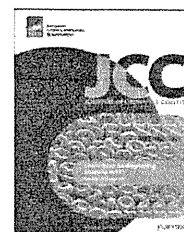
**Conflict of interest** The authors declare that they have no conflict of interest.

## References

- Isaacson PG. Mucosa-associated lymphoid tissue lymphoma. *Semin Hematol.* 1999;36:139–47.
- Isaacson PG. Gastrointestinal lymphomas of T- and B-cell types. *Mod Pathol.* 1999;12:151–8.
- Wotherspoon AC, Doglioni C, Diss TC, et al. Regression of primary low-grade B-cell gastric lymphoma of mucosa-associated lymphoid tissue type after eradication of *Helicobacter pylori*. *Lancet.* 1993;342:575–7.
- Wotherspoon AC. *Helicobacter pylori* infection and gastric lymphoma. *Br Med Bull.* 1998;54:79–85.
- Wotherspoon AC. Gastric lymphoma of mucosa-associated lymphoid tissue and *Helicobacter pylori*. *Annu Rev Med.* 1998;49:289–99.
- Romaguera J, Hagemester FB. Lymphoma of the colon. *Curr Opin Gastroenterol.* 2005;21:80–4.
- Ahlawat S, Kanber Y, Charabaty-Pishvaian A, et al. Primary mucosa-associated lymphoid tissue (MALT) lymphoma occurring in the rectum: a case report and review of the literature. *South Med J.* 2006;99:1378–84.
- Tanaka S, Ohta T, Kaji E, et al. EMR of mucosa-associated lymphoid tissue lymphoma of the rectum. *Gastrointest Endosc.* 2003;57:956–9.
- Grunberger B, Wohrer S, Streubel B, et al. Antibiotic treatment is not effective in patients infected with *Helicobacter pylori* suffering from extragastric MALT lymphoma. *J Clin Oncol.* 2006;24:1370–5.
- Matsumoto T, Iida M, Shimizu M. Regression of mucosa-associated lymphoid-tissue lymphoma of rectum after eradication of *Helicobacter pylori*. *Lancet.* 1997;350:115–6.
- Matsumoto T, Shimizu M, Iida M, et al. Primary low-grade, B-cell, mucosa-associated lymphoid tissue lymphoma of the colorectum: clinical and colonoscopic features in six cases. *Gastrointest Endosc.* 1998;48:501–8.
- Inoue F, Chiba T. Regression of MALT lymphoma of the rectum after anti-*H. pylori* therapy in a patient negative for *H. pylori*. *Gastroenterology.* 1999;117:514–5.
- Niino D, Yamamoto K, Tsuruta O, et al. Regression of rectal mucosa-associated lymphoid tissue (MALT) lymphoma after antibiotic treatments. *Pathol Int.* 2010;60:438–42.
- Hisabe T, Imamura K, Furukawa K, et al. Regression of CD5-positive and *Helicobacter pylori*-negative mucosa-associated lymphoid tissue lymphoma of the rectum after administration of antibiotics: report of a case. *Dis Colon Rectum.* 2002;45:1267–70.
- Nakase H, Okazaki K, Ohana M, et al. The possible involvement of micro-organisms other than *Helicobacter pylori* in the development of rectal MALT lymphoma in *H. pylori*-negative patients. *Endoscopy.* 2002;34:343–6.
- Hori K, Suguro M, Koizuka H, et al. Disappearance of rectal mucosa-associated lymphoid tissue lymphoma following antibiotic therapy. *Dig Dis Sci.* 2004;49:413–6.
- Kikuchi Y, Matsui T, Hisabe T, et al. Deep infiltrative low-grade MALT (mucosal-associated lymphoid tissue) colonic lymphomas that regressed as a result of antibiotic administration: endoscopic ultrasound evaluation. *J Gastroenterol.* 2005;40:843–7.
- Ahlawat S, Haddad N, Kanber Y, et al. Primary mucosa-associated lymphoid tissue lymphoma occurring in the rectum. *Gastrointest Endosc.* 2005;62:443–4. (discussion 444).
- Dohden K, Kaizaki Y, Hosokawa O, et al. Regression of rectal mucosa-associated lymphoid tissue lymphoma but persistence of *Helicobacter pylori* infection of gastric mucosa after administration of levofloxacin: report of a case. *Dis Colon Rectum.* 2004;47:1544–6.

Available online at [www.sciencedirect.com](http://www.sciencedirect.com)

SciVerse ScienceDirect



## Olfactomedin-4 is a glycoprotein secreted into mucus in active IBD<sup>☆</sup>

Michael Gersemann<sup>a, b, \*</sup>, Svetlana Becker<sup>b</sup>, Sabine Nuding<sup>b</sup>, Lena Antoni<sup>b</sup>, German Ott<sup>c</sup>, Peter Fritz<sup>c</sup>, Naohide Oue<sup>d</sup>, Wataru Yasui<sup>d</sup>, Jan Wehkamp<sup>a, b</sup>, Eduard F. Stange<sup>a</sup>

<sup>a</sup> Department of Internal Medicine I, Robert Bosch Hospital, Stuttgart, Germany

<sup>b</sup> Dr. Margarete Fischer-Bosch Institute of Clinical Pharmacology, Stuttgart and University of Tübingen, Germany

<sup>c</sup> Department of Pathology, Robert Bosch Hospital, Stuttgart, Germany

<sup>d</sup> Department of Molecular Pathology, Hiroshima University Graduate School of Biomedical Science, Hiroshima, Japan

Received 12 August 2011; received in revised form 28 September 2011; accepted 28 September 2011

### KEYWORDS

Inflammatory bowel disease;  
Olfactomedin-4;  
Intestinal stem cell marker;  
Defensins;  
Mucins;  
Mucus

### Abstract

**Background:** Olfactomedin-4 (OLFM4) is a glycoprotein characteristic of intestinal stem cells and apparently involved in mucosal defense of the stomach and colon. Here we studied its expression, regulation and function in IBD.

**Methods:** The expression of OLFM4, mucins Muc1 and Muc2, the goblet cell differentiation factor Hath1 and the proinflammatory cytokine IL-8 was measured in inflamed or noninflamed colon in IBD patients and controls. OLFM4 protein was located by immunohistochemistry, quantified by Dot Blot and its binding capacity to defensins HBD1-3 was investigated. The influence of bacteria with or without the Notch blocker dibenzazepine (DBZ) and of several cytokines on OLFM4 expression was determined in LS174T cells.

**Results:** OLFM4 mRNA and protein were significantly upregulated in inflamed CD (4.3 and 1.7-fold) and even more pronounced in UC (24.8 and 3.7-fold). OLFM4 expression was correlated to IL-8 but not to Hath1. In controls immunostaining was restricted to the lower crypts but in inflamed IBD it expanded up to the epithelial surface including the mucus. OLFM4 bound to HBD1-3 without profoundly inactivating these defensins. In LS174T-cells OLFM4 mRNA was significantly augmented after incubation with *Escherichia coli* K12, *Escherichia coli* Nissle and *Bacteroides vulgatus*. DBZ downregulated OLFM4 expression and blocked bacterial induction whereas IL-22 but not TNF- $\alpha$  was stimulatory.

<sup>☆</sup> Conference presentation: DDW 2011, Chicago, USA (poster).

\* Corresponding author at: Robert Bosch Hospital, Internal Medicine I, Auerbachstr. 110, D-70376 Stuttgart, Germany. Tel.: +49 711 81015912; fax: +49 711 81013793.

E-mail address: michael.gersemann@rbk.de (M. Gersemann).

**Conclusions:** OLFM4 is overexpressed in active IBD and secreted into mucus. The induction is triggered by bacteria through the Notch pathway and also by the cytokine IL-22. OLFM4 seems to be of functional relevance in IBD as a mucus component, possibly by binding defensins.

© 2011 European Crohn's and Colitis Organisation. Published by Elsevier B.V. All rights reserved.

## 1. Introduction

In both inflammatory bowel diseases (IBD) the chronic inflammation is mediated by an immune response directed against commensal bacteria, possibly triggered by a disproportionate immune response toward these microbes that damages the mucosa.<sup>1</sup> On the other hand, there is increasing evidence for a primary role of a defective mucosal barrier in Crohn's disease (CD) and ulcerative colitis (UC).<sup>2–4</sup> Bacteria from the lumen massively contaminate the mucus layer<sup>5</sup> which is normally sterile in the bottom stratum.<sup>6</sup> Some bacteria are epithelial adherent<sup>5,7</sup> or may even invade the sub-epithelial space<sup>5,8</sup> and thus trigger an immune response.

The mucosal barrier is a multilayer structure composed of the mucus layer<sup>6</sup> and its origin, the epithelium. In the large intestine the key secretory cells are the goblet cells. They produce various mucins forming the mucus layer which is acting as a physical and chemical barrier against commensals and pathogens.<sup>9</sup> The colonic epithelium also produces antimicrobial peptides which are ultimately secreted into the mucus.<sup>10,11</sup> The more important colonic peptides, the  $\beta$ -defensins, are characterized by a broad antimicrobial activity against a variety of gram-positive and gram-negative bacteria preventing luminal microbes to enter the lower mucus layer and attack the epithelium.<sup>12</sup>

This intestinal protective barrier mediated by mucus and defensins is disturbed in IBD. In CD, the expression of the antimicrobial peptides is compromised enabling the bacteria to invade the mucosa and thus trigger inflammation.<sup>3,13</sup> In case of colonic involvement, CD is linked to a diminished expression of HBD1 independent of inflammation.<sup>14</sup> In UC, the mucus layer is thinner than normal and may even be missing.<sup>15,16</sup> This is accompanied by a diminished mucin synthesis,<sup>17–21</sup> which is apparently related to a failure in the differentiation of intestinal stem cells toward goblet cells.<sup>17</sup> This differentiation is governed by the key transcription factor *Hath1* which is correlated with mucin synthesis.<sup>17</sup>

Olfactomedin-4 (OLFM4) is an olfactomedin domain-containing protein which was found preferentially in the human gastrointestinal tract.<sup>22–24</sup> The function of OLFM4 in the digestive tract is probably complex. OLFM4 may be an important part of the gastrointestinal mucosal surface and therefore play a role in its defense.<sup>25</sup> For instance, OLFM4 is known to create large polymers stabilized by disulfide bonds,<sup>25</sup> similar to mucins.<sup>9</sup> Moreover, it was demonstrated to interact with cell surface cadherin and lectins facilitating cell adhesion.<sup>26</sup> A role of OLFM4 in epithelial defense was concluded from an upregulation in a mouse primary gastric epithelial cell line GSM06 incubated with *Helicobacter pylori*,<sup>27</sup> as well as in *H. pylori* infected patients in vivo.<sup>28</sup> Finally, in addition to LGR5<sup>29</sup> also OLFM4 was found to be a small and large intestinal marker for crypt stem cells in humans.<sup>30</sup>

However, little is known about its relevance in the colon. Shinozaki et al. found OLFM4 transcripts to be significantly upregulated in the epithelium in active vs. inactive UC but its precise function remained unclear.<sup>31</sup> In the present study we attempted to better define the role of OLFM4 in the pathogenesis of IBD and suggest that this peptide acts as an inflammation induced mucus component binding defensins.

## 2. Material and methods

### 2.1. Patients

The diagnosis of CD and UC was based on classical clinical, radiological and endoscopic findings.<sup>32,33</sup> Endoscopic biopsies were immediately snap-frozen in liquid nitrogen. All patients gave their written informed consent and the study was approved by the ethical committee of the University of Tübingen (Germany).

For real-time PCR analysis biopsies from the colonic sigma were obtained in a total of 160 individuals, who underwent routine colonoscopy for various indications, such as colon cancer screening, IBD, diarrhea or obstipation. Thirty-three of these biopsies were classified as healthy controls, 72 were from CD patients (36 noninflamed and 36 inflamed samples) and 55 had the diagnosis of UC (28 noninflamed and 27 inflamed samples). All samples were collected at the Robert Bosch Hospital (Stuttgart, Germany) and the intensity of the flare was clinically evaluated in these patients using the Colitis Activity Index (CAI) for UC and the Crohn's disease activity index (CDAI) for CD.

Immunostaining was performed in formalin-fixed or Carnoy-fixed paraffin-embedded colonic tissue. A total of 18 formalin-fixed colonic resections (6 controls, 6 inflamed CD and 6 inflamed UC samples) and 10 Carnoy-fixed rectal biopsies (5 inflamed CD and 5 inflamed UC samples) were investigated. For Dot Blot analysis, sigma biopsies of 4 controls, 4 inflamed CD and 4 inflamed UC patients, as well as mucus extracts obtained by colonoscopic brushings from 3 controls, 3 inflamed CD and 3 inflamed UC samples were collected. Brushings were performed by gently scrubbing the rectal mucosa with an endoscopic brush, removing the endoscope from the rectum and, outside the patient, the brush was cut with scissors and snap frozen in liquid nitrogen.

### 2.2. RNA isolation and reverse transcription

The frozen tissues were mechanically disrupted and total RNA was isolated using TRIzol reagent (Invitrogen, Karlsruhe, Germany). RNA quality was checked with the Agilent RNA 6000 Nano Kit (Agilent Technologies, Santa Clara, CA, USA). 500 ng of total RNA was reverse transcribed with AMV reverse transcriptase according to the supplier's protocol

(Promega, Mannheim, Germany). RNA preparations were used for real-time PCR analysis.

### 2.3. Protein preparation

Frozen sigmoid biopsies were pulverized with a pestle in liquid nitrogen. Proteins were extracted under gentle agitation for 90 min diluted in 100  $\mu$ l homogenization buffer (50 mM Tris HCl, 250 mM sucrose, 1 mM EDTA, pH 7.6). Extracts were centrifuged for 20 min (13200 g, 4 °C) and the supernatants were immediately snap-frozen in liquid nitrogen. Mucus extracts were incubated for 2 h in 300  $\mu$ l 5% acetic acid following a centrifugation for 10 min (7000 g, 4 °C). Then the supernatants were extracted and dried in a vacuum concentrator. Pellets were diluted in 80  $\mu$ l 0.01% acetic acid and immediately snap-frozen in liquid nitrogen. Protein content in biopsies and mucus extracts was measured using a Bicinchoninic Acid Protein Assay (Smith) as described previously.<sup>34</sup> Isolated proteins were used for Dot Blot analyses.

### 2.4. Quantitative real-time reverse transcriptase PCR

For mRNA quantification, real-time PCR was carried out in a SYBR Green fluorescence temperature cycler (LightCycler®, Roche Diagnostics, Mannheim, Germany). Single-stranded cDNA (or gene-specific plasmids as controls) corresponding to 10 ng of RNA conducted as a template with specific oligonucleotide primer pairs (Table 1) as described previously.<sup>13</sup> All primers were tested for specific binding to the sequence of interest using BLAST. Plasmids for each product were generated with the TOPO TA Cloning Kit (Invitrogen, Carlsbad, CA, USA) according to the supplier's protocol. PCR-amplified DNA fragments were confirmed by sequencing. Internal standard curves were produced by serial dilution of the correctly sequenced plasmids. The mRNA data were normalized to  $\beta$ -actin mRNA.

### 2.5. Immunohistochemistry

A monoclonal antibody directed against OLFM4 (N212) was produced by W.Y. in the Department of Molecular Pathology, Hiroshima University Graduate School of Biomedical Science, Hiroshima, Japan; proof for its specificity has previously been published.<sup>35</sup> Immunostaining for OLFM4 was performed using a two-step immunoperoxidase technique (EnVision™, Dako, Glostrup, Denmark) as described previously.<sup>36</sup> Antigen retrieval was performed by heating for 30 min in a steamer

(pH 9). Then, sections were incubated for 1 h with the primary anti-OLFM4 antibody diluted 1:100 in TBST (20 mM Tris-Base (pH 7.4), 0.14 M NaCl, 0.1% Tween 20). Visualization was performed using a detection kit as outlined by the supplier (Dako, Glostrup, Denmark: horse-radish-peroxidase (HRP)-labeled secondary antibody, detection with 3'-diaminobenzidine tetrahydrochloride). Sections were counterstained with hematoxylin. The grade of inflammation was blindly evaluated in H & E stained sections by an experienced pathologist blinded to the immunohistochemical and molecular biological results.

### 2.6. Dot Blot analysis

The specificity of the anti-OLFM4 antibody (N212) was tested in Western Blot experiments using human sigma biopsies. We found a clear signal at 57 kDa in inflamed UC samples which is less intense in inflamed CD and uninflamed controls (data not shown). Due to the limited protein amounts obtained by a single biopsy, we decided to switch to the Dot Blot technique which needs less total protein amounts as compared to the Western Blot. Therefore, 10  $\mu$ g of total protein was transferred to 0.45 mg pore size nitrocellulose membranes (Schleicher & Schuell, Keene, NH, USA) and blocked with 5% skimmed milk powder in TBST for 1 h. The membranes were washed and incubated for 1 h with the primary anti-OLFM4 antibody (diluted 1:1000 in 5% skimmed milk powder in TBST). Then, the membranes were washed again and treated for 1 h with the secondary HRP-conjugated goat anti-mouse immunoglobulin G antibody (Immuno Research Laboratories, West Grove, PA, USA; diluted 1:5000 in 5% skimmed milk powder in TBST). Protein detection was performed using the Amersham™ ECL Plus Western Blotting Detection System (GE Healthcare, Chalfont St Giles, UK). Signals were visualized with a chemiluminescence camera charge-coupled device LAS-1000 (Fuji, Tokyo, Japan). Densitometric analysis was performed with AIDA 2.1 software (Raytest, Straubenhardt, Germany).

After 24 h primary and secondary antibodies were removed from the membranes by incubation for 30 min in Restore™ Western Blot Stripping Buffer (Thermo Scientific, Rockford, IL, USA). Then, Dot Blot analysis was performed for  $\beta$ -actin on the same membranes. The primary  $\beta$ -actin antibody (Sigma, Deisenhofen, Germany) and also the secondary HRP-conjugated goat anti-mouse immunoglobulin G antibody (Immuno Research Laboratories, West Grove, PA, USA) were diluted 1:5000 in 5% skimmed milk powder in TBST. Detection of  $\beta$ -actin was performed as described above. In sigma biopsies, OLFM4 protein content was

**Table 1** Oligonucleotide primer pairs used for PCR measurements.

Product	Forward primer (5' -> 3')	Reverse primer (5' -> 3')
$\beta$ -actin	GCCAACCGCGAGAAGATGA	CATCACGATGCCAGTGGTA
IL-8	ATGACTTCCAAGCTGGCCGTGGC	TCTCAGCCCTCTTCAAAACTTC
OLFM4	TGCCATTGCGCCGAGAAATCGTGGCTCT	TCACCACACCACCATGACCACAGCTCC
Muc1	AGACGTCAGCGTGAGTGATG	CAGCTGCCCGTAGTCTTTC
Muc2	ACCCGCACTATGTCACTTC	GGGATCGCAGTGGTAGTTGT
Hath1	CGAGAGGCATCCCGTCTAC	TCCGGGAATGTAGCAATA

Please cite this article as: Gersemann M, et al. Olfactomedin-4 is a glycoprotein secreted into mucus in active IBD. *Journal of Crohn's and Colitis* (2011), doi:10.1016/j.crohns.2011.09.013



normalized to  $\beta$ -actin by dividing the densitometric intensity (LAU) of OLFM4 through the LAU of  $\beta$ -actin in the same biopsy. Notably, OLFM4 and  $\beta$ -actin, were exposed for the same time period (5 min).

### 2.7. HBD1-3/OLFM4 binding assay

To investigate the possibility that OLFM4 binds to the major colonic defensins, we developed an HBD1-3/OLFM4 binding assay. Therefore, 96 well plates (Nunc, Roskilde, Denmark) were coated for 3 times in triplicates overnight at 4 °C with 5  $\mu$ g HBD1, HBD2 or HBD3 (Peptanova, Sandhausen, Germany) or 5  $\mu$ g bovine serum albumin (BSA, Sigma, Deisenhofen, Germany) per well in 100  $\mu$ l coating buffer (50 mM NaHCO<sub>3</sub>/Na<sub>2</sub>CO<sub>3</sub>, pH 9.6). As a control, 100  $\mu$ l coating buffer alone was used. The next day the wells were washed with TBST and blocked with 5% skimmed milk powder in TBST for 1 h. After repeatedly washing with TBST, the wells were incubated overnight at 4 °C with 0, 2 or 6  $\mu$ g OLFM4 (Sino Biological, Beijing, China) in 100  $\mu$ l 5% skimmed milk powder in TBST. Then, wells were washed again and incubated with the anti-OLFM4 antibody diluted 1:500 in 5% skimmed milk powder in TBST for 1 h. After repeatedly washing, wells were incubated with a HRP-labeled secondary antibody (Dako, Glostrup, Denmark) for 30 min. Again, wells were washed and thereafter incubated with 200  $\mu$ l 2,2'-azino-bis-3-ethylthiazoline-6-sulphonic acid (ABTS, Sigma, Deisenhofen, Germany) for 10 min. Photometric visualization was carried out with Wallac Victor™ 1420 Multitable Counter (Waltham, MA, USA) at 405 nm wave length.

### 2.8. Flow cytometric assay

Antimicrobial activity was measured with a flow cytometric test as described previously.<sup>37</sup> Briefly, suspensions of *Escherichia coli* ATCC 25922 were grown overnight in Schaedler Broth (BD, Sparks, MD, USA) diluted 1:6 with sterile distilled water at 37 °C. Subsequently 1.5  $\times$  10<sup>6</sup> mid-logarithmic-phase bacteria/ml in Schaedler Broth 1:6 in a final volume of 100  $\mu$ l were incubated with 5  $\mu$ g HBD1, HBD2 or HBD3 (Peptanova, Sandhausen, Germany) and 2 or 6  $\mu$ g recombinant human OLFM4 (Sino Biological, Beijing, China) at 37 °C. Since OLFM4 is diluted 1  $\mu$ g/ $\mu$ l in OLFM4-solvent buffer (0.2  $\mu$ m filtered solution of PBS, pH 7.4, 3.2% glycerol, 8% trehalose, 8% mannitol) by the company, bacteria were also incubated with 5  $\mu$ g HBD1-3 and 2 or 6  $\mu$ l OLFM4 solution buffer alone (obtained by the company) for control experiments. Three independent experiments were performed in triplicates. After 90 min, 1  $\mu$ g/ml of the membrane potential sensitive dye DiBAC<sub>4</sub>(3) (bis-(1,3-dibutylbarbituric acid) trimethine oxonol; Invitrogen, Carlsbad, CA, USA) was added. After 10 min of incubation, the samples were centrifuged for 10 min at 4500 g and the bacterial pellets were resuspended in 300  $\mu$ l phosphate buffered saline (pH 7.4). With a FACSCalibur™ flow cytometer (BD, Sparks, MD, USA) 10000 events of each sample were analyzed for light scattering and green fluorescence. Antimicrobial activity was determined as percentage of fluorescent depolarized bacteria.

### 2.9. Cell culture experiments

The colon adenocarcinoma cell line LS174T (American Type Culture Collection, Manassas, USA) was cultivated in Dulbecco's modified Eagle medium (DMEM, Gibco Life Technologies, Eggenstein, Germany) completed with 10% fetal calf serum (FCS, PAA Laboratories, Pasching, Austria), 1% non essential amino acids (Gibco Life Technologies, Eggenstein, Germany), 1% penicillin/streptomycin (Gibco Life Technologies, Eggenstein, Germany) and 1% sodium pyruvate (Gibco Life Technologies, Eggenstein, Germany) in a humidified atmosphere at 37 °C and 5% CO<sub>2</sub>. For experiments, cells were seeded for at least 3 times in triplicates into 12-well culture plates (Becton Dickinson, Franklin Lakes, New Jersey, USA) at a density of 0.65  $\times$  10<sup>6</sup> per well. At about 70% confluence, cells were washed with phosphate-buffered saline (Gibco Life Technologies, Eggenstein, Germany) and incubated in FCS- and antibiotic-free DMEM for 12 h.

Then, cells were incubated with *E. coli* K12, *E. coli* Nissle, *Bacteroides vulgatus*, *Symbioflor* G1/G2/G3, *Lactobacillus fermentum* and *acidophilus*, as well as *Bifidobacterium longum*, *breve* and *adolescentis* for 6 and 24 h. All *E. coli* strains and *B. vulgatus* were cultivated under aerobic, *Lactobacilli* and *Bifidobacteria* under anaerobic conditions as previously described.<sup>38</sup> Bacteria were killed per heat inactivation in a water bath at 65 °C for 1 h. Then, bacteria were washed with PBS and adjusted to a density of 3  $\times$  10<sup>8</sup> cells/ml with FCS- and antibiotic-free DMEM. To investigate the possible role of the Notch signaling pathway in regulating OLFM4, cells were incubated for 6 and 24 h with the  $\gamma$ -secretase inhibitor dibenzazepine (DBZ, Axon Medchem, Groningen, Netherlands) in a concentration of 1  $\mu$ M (in 0.1% DMSO in DMEM) in the absence or presence of *E. coli* Nissle. LS174T cells were also treated with 10 ng/ml TNF- $\alpha$  (Sigma, Deisenhofen, Germany), 100 ng/ml IL-22 (Sigma, Deisenhofen, Germany), 10 ng/ml IL-4 (Sigma, Deisenhofen, Germany) and 10 ng/ml IL-13 (Sigma, Deisenhofen, Germany) for 6, 12 and 24 h. At the end of experiments cells were washed with PBS and mRNA was isolated using RNeasy Mini Kit (Qiagen, Venlo, Netherlands) according to the supplier's protocol.

### 2.10. Statistics

Statistical analyses were performed and all graphs were generated with the GraphPad Prism version 4.0 software using the Mann-Whitney test. In case of the PCR measurements in human sigma biopsies, Bonferroni correction was also done. Spearman's rank analysis was performed for nonparametric correlation between the different subgroups of the quantitative real-time PCR results. Values of p < 0.05 were considered to be statistically significant. Data are presented in box and whiskers (means).

## 3. Results

### 3.1. OLFM4 and mucins are differentially expressed in inflamed IBD

In colonic biopsies transcripts of the proinflammatory cytokine IL-8 (Fig. 1A) were equally enhanced in inflamed CD

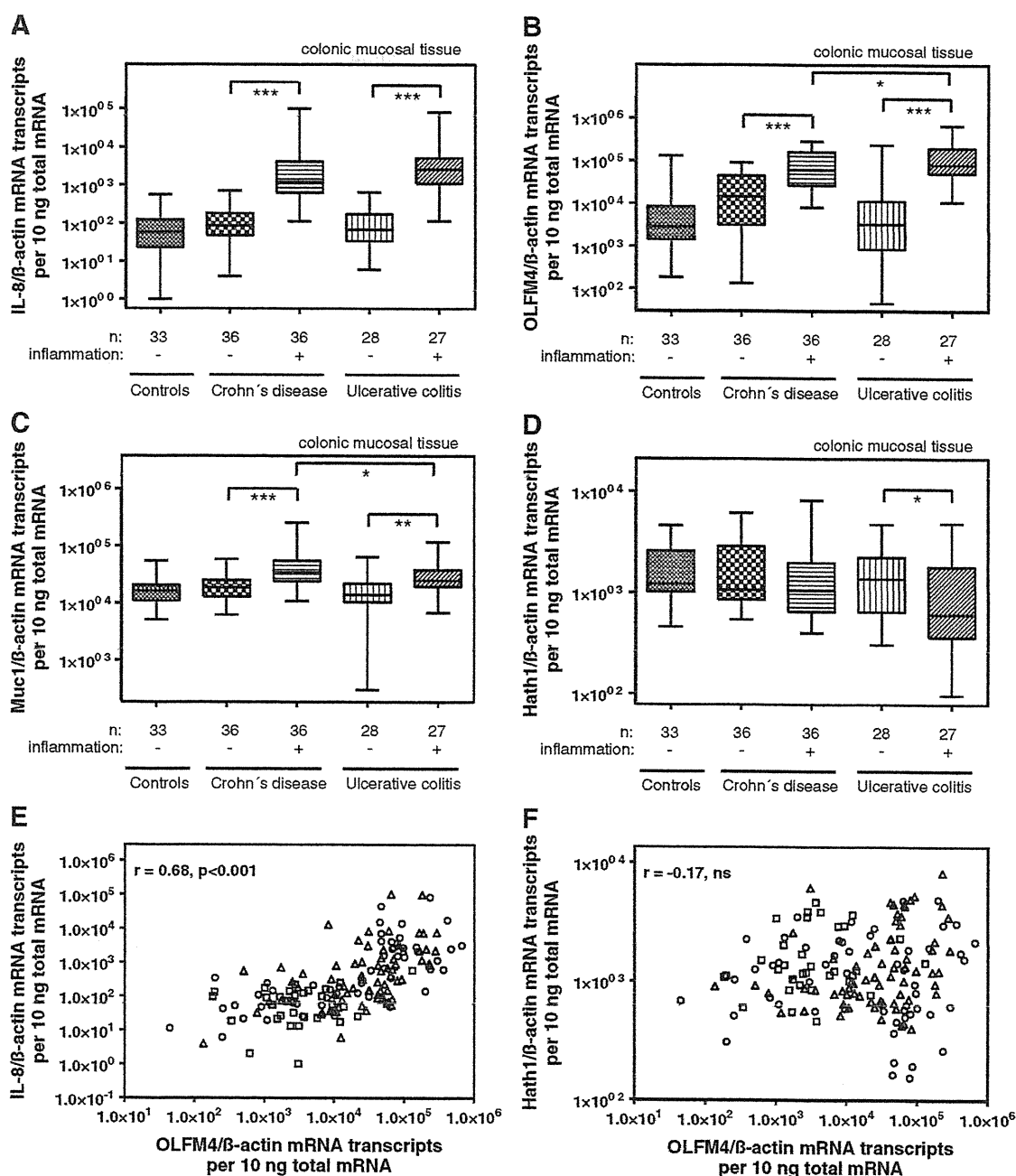


**Figure 1** IL-8, OLFM4, Muc1 and Hath1 expression in controls and IBD mucosa: IL-8 transcripts are enhanced in inflamed vs. noninflamed CD and UC without significant differences between both diseases (A). OLFM4 mRNA was significantly more induced in CD than UC (B). Muc1 transcripts are augmented more in inflamed vs. noninflamed CD than in UC (C). Hath1 mRNA is significantly downregulated in inflamed UC (D). OLFM4 is highly correlated with IL-8 (E,  $r = 0.68$  for all samples,  $p < 0.001$ ) but not with Hath1 (F,  $r = -0.17$  for all samples, ns; squares = controls, triangles = CD, circles = UC; \*,  $p < 0.05$  (these significances are lost after Bonferroni correction), \*\*,  $p < 0.01$ , \*\*\*,  $p < 0.001$ ).

(14-fold,  $p < 0.001$ ) and UC (38-fold,  $p < 0.001$ ) compared to the respective noninflamed samples. In controls and noninflamed IBD samples IL-8 expression was comparably low. The grade of histological inflammation was similar in both inflamed IBD entities (inflammation score for controls: 1.0, for CD: 7.2 and for UC: 7.0). The CAI was 2.6 for the

noninflamed UC group and 12.1 for the inflamed UC patients. The CDAI was 188 in case of noninflamed colonic CD and 237 in inflamed colonic CD patients.

OLFM4 mRNA (Fig. 1B) was significantly induced in inflamed CD (4.3-fold,  $p < 0.001$ ) and UC (24.8-fold,  $p < 0.001$ ) vs. noninflamed biopsies. This upregulation was clearly

higher in inflamed UC than in inflamed CD samples (5.8-fold,  $p=0.04$ ). Again, controls and noninflamed samples were in the same range. Immunostaining for OLFM4 in normal human colonic tissues was confined to the lower third of crypts but expanded during inflammation up to the epithelial surface (Fig. 2). The OLFM4 protein content normalized to  $\beta$ -actin as determined by Dot Blot analysis (Fig. 3) was also clearly augmented in inflamed CD (1.7-fold,  $p=0.03$ ) and UC (3.7-fold,  $p=0.03$ ) as compared to controls. Again, this induction was numerically more pronounced in inflamed UC as compared to inflamed CD (ns).

Muc1 transcripts (Fig. 1C) were also significantly augmented in inflamed CD (1.9-fold,  $p<0.001$ ) and UC (1.8-fold,  $p=0.002$ ) samples as compared to controls. In contrast to OLFM4, this induction was less significant in inflamed UC

than in inflamed CD biopsies ( $p=0.03$ ). Controls and noninflamed samples exhibited a comparable expression. Muc2 mRNA levels did not show significant differences between the 5 subgroups (data not shown). Hath1 expression (Fig. 1D) was significantly lower in inflamed vs. noninflamed UC (0.7-fold,  $p=0.02$ ) but not CD. Transcripts of OLFM4 correlated significantly with IL-8 (Spearman  $r: 0.68$ ,  $p<0.001$ , Fig. 1E) and Muc1 ( $r: 0.57$ ,  $p<0.001$ ) but not with Hath1 ( $r: -0.17$ , ns, Fig. 1F).

### 3.2. OLFM4 is secreted into the mucus and binds to $\beta$ -defensins HBD1-3

Since OLFM4 is upregulated in inflamed IBD and staining was found up to the epithelial surface, we searched for OLFM4 protein in human mucus following Carnoy-fixation. Indeed, rectal IBD biopsies showed a positive immunostaining for OLFM4 in the crypt lumen (Fig. 4A) as well as in the surface mucus (Fig. 4B), implying the secretion of OLFM4 by epithelial cells into the mucus. This observation was confirmed in rectal mucus extracts, which were obtained by colonoscopic brushings and analyzed with the Dot Blot technique (Fig. 4C): OLFM4 protein was found in the mucus of patients with inflamed CD and even more pronounced in patients with inflamed UC, whereas noninflamed mucus controls were almost negative. As expected,  $\beta$ -actin was only marginally detectable in mucus showing that these extracts were almost free of cell detritus.

The defensins HBD1-3 are positively charged and also secreted into the mucus<sup>10</sup> whereas OLFM4 has a negative charge. Therefore, we tested the ability of recombinant OLFM4 to bind HBD1-3 preabsorbed to plastic wells. In contrast to no binding to BSA, OLFM4 preferentially bound to preabsorbed HBD3 > HBD2 and > HBD1 (Fig. 5). Next, we checked the antimicrobial activity of HBD1-3 in the absence and presence of OLFM4. The coincubation of defensins with OLFM4 at 2 and 6  $\mu\text{g/ml}$  was associated with a limited reduction of the antimicrobial activity in case of HBD1 from 66% to 58% (2  $\mu\text{g/ml}$ , ns) and 47% to 39% (6  $\mu\text{g/ml}$ , ns), in case of HBD2 from 69% to 54% (2  $\mu\text{g/ml}$ , ns) and from 57% to 41% (6  $\mu\text{g/ml}$ , ns) and in case of HBD3 from 71% to 65% (2  $\mu\text{g/ml}$ , ns) and from 55% to 51% (6  $\mu\text{g/ml}$ , ns).

### 3.3. Bacteria and IL-22 induce OLFM4 expression in LS174T cells

The mucin producing colon adenocarcinoma cell line LS174T was incubated with heat killed *E. coli* K12, *E. coli* Nissle, *B. vulgatus*, *Symbioflor* G1/G2/G3, *L. fermentum* and *acidophilus*, as well as *B. longum*, *breve* and *adolescentis*. An incubation for 24 h with *E. coli* K12 (2.8-fold induction,  $p=0.009$ ), *E. coli* Nissle (2.5-fold,  $p=0.02$ ) and *B. vulgatus* (1.9-fold,  $p=0.02$ ) led to a significant increase of OLFM4 expression in these LS174T cells. In contrast, OLFM4 was unaffected by heat killed *Symbioflor* G1/G2/G3, *L. fermentum* and *acidophilus*, as well as *B. longum*, *breve* and *adolescentis* (data not shown).

In addition, LS174T cells showed a significant time-dependent increase of OLFM4 expression following a treatment with 100 ng/ml IL-22 (3.4-fold after 6 h,  $p=0.04$ ; 5.3-fold after 12 h,  $p=0.01$ ; 9.1-fold after 24 h,  $p=0.01$ ). In

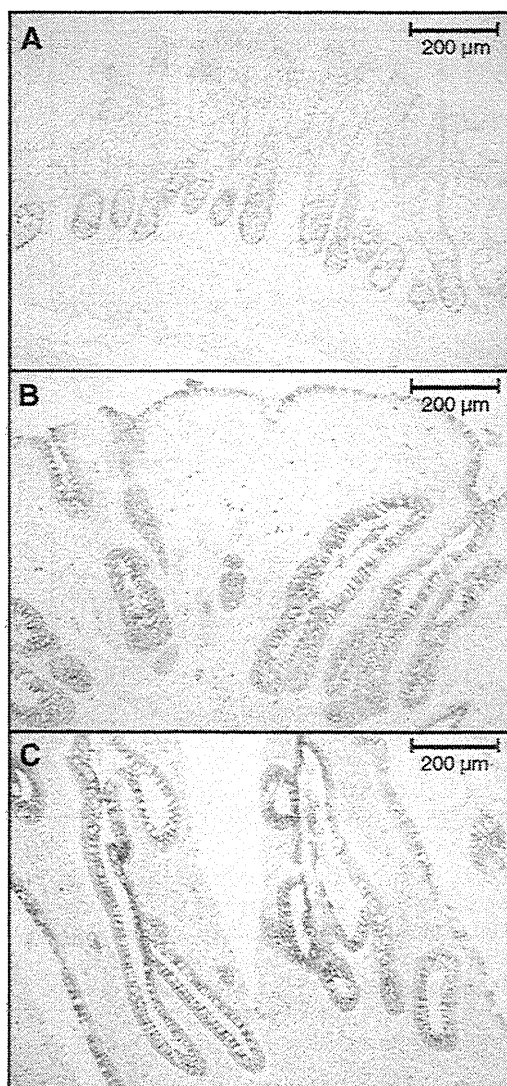


**Figure 2** OLFM4 immunostaining in controls and IBD mucosa: OLFM4 staining is located in the lower third of the crypt in control samples (A, magnification 100-fold) and expanded up to the epithelial surface during inflammation (B = inflamed CD, C = inflamed UC, magnification 100-fold).

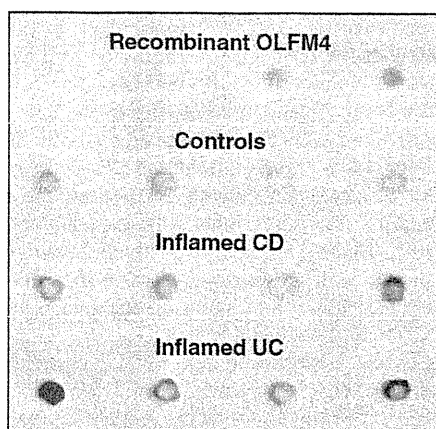


**Figure 3** OLFM4 Dot Blot analysis in controls and IBD mucosa: OLFM4 protein is significantly increased in inflamed CD and even more pronounced in inflamed UC biopsy samples as compared to controls (top lane: recombinant OLFM4 in increasing amounts from left to right: 0.05, 0.1, 0.5 and 1  $\mu$ g).

contrast, incubation with TNF- $\alpha$  (0.8–1.4-fold increase, ns), IL-4 (0.7–1.0-fold, ns) and IL-13 (0.7–1.3-fold, ns) did not influence OLFM4 expression.

### 3.4. OLFM4 is regulated by the Notch pathway

To elucidate the mechanism by which bacteria can influence the level of OLFM4 expression, we investigated the involvement of the Notch pathway in the regulation of OLFM4. Accordingly, LS174T cells were treated with heat inactivated *E. coli Nissle* in the presence or absence of  $\gamma$ -secretase inhibitor dibenzazepine (DBZ, Fig. 6). In the absence of

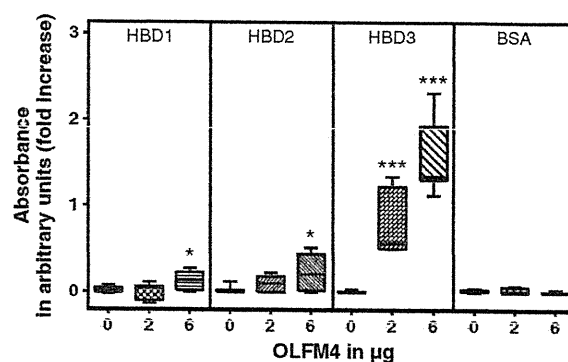


**Figure 5** OLFM4 binding to HBD1-3: Coincubation of OLFM4 with HBD1-3, but not bovine serum albumin (BSA), resulted in a dose dependent increase of OLFM4 absorption (\*:  $p < 0.05$ , \*\*\*:  $p < 0.001$ ).

bacteria DBZ treatment resulted in a significant downregulation of OLFM4 transcripts to 11% after 24 h ( $p = 0.004$ ). The coincubation with *E. coli Nissle* and DBZ for 24 h nearly completely blocked the 2.4 fold induction by *E. coli Nissle* ( $p = 0.004$ ).

### 4. Discussion

OLF4 is still an enigmatic, ambiguous protein. On the one hand, the protein marks intestinal stem cells,<sup>30</sup> on the other hand it also seems to be important in host defense during gastric and colonic infection and inflammation.<sup>25–27</sup> In particular, the regulation and function of OLF4 in the colon are still not completely understood.<sup>25</sup>

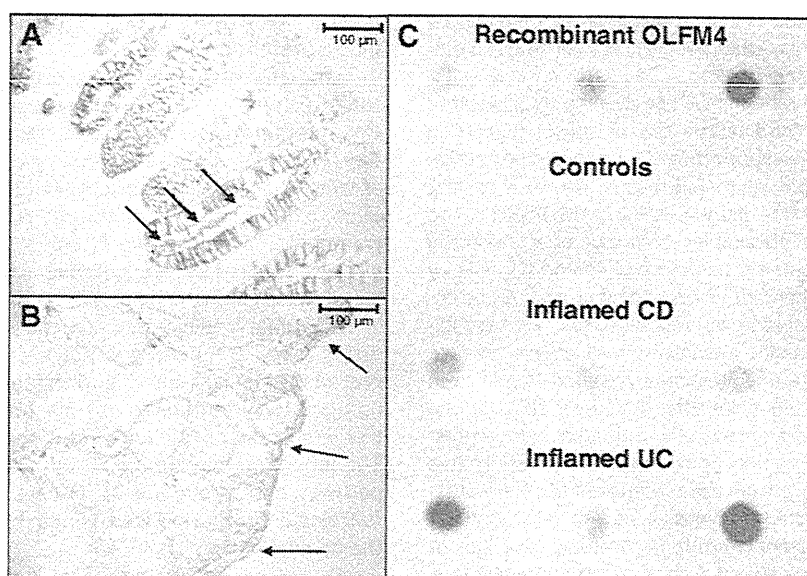


**Figure 4** Secreted OLFM4 in controls and IBD mucus: OLFM4 is found in the crypt lumen (A = CD, arrows, magnification 200-fold) and also in the surface mucus (B = UC, arrows, magnification 200-fold). Dot Blot analysis demonstrates OLFM4 in rectal mucus extracts (C, top lane: recombinant OLFM4 in increasing concentrations from left to right: 0.05, 0.1 and 0.5  $\mu$ g).